DOI: https://doi.org/10.1016/j.jeurceramsoc.2020.09.016

Innovative strategy for designing proton conducting ceramic tapes and multilayers for energy applications

Elisa Mercadelli*, Angela Gondolini, Daniel Montaleone, Paola Pinasco, Alessandra Sanson

National Council of Research, Institute of Science and Technology for Ceramics, (CNR-ISTEC), Via Granarolo 64, 48018, Faenza, Italy

* Corresponding author: elisa.mercadelli@istec.cnr.it, Tel.: +39 0546699743, fax: +390546699799

Abstract

Aim of this work is to present, for the first time, the use of Dynamic Mechanical Analysis as a tool to characterize the thermo-mechanical behavior of green tapes defining the process conditions for the subsequent lamination step. This method was applied on tapes of protonic conductors, key-materials for different applications in the energy sector, from gas separation membranes to solid oxide fuel cells and electrolyzers. The pore former (rice starch) content was found to considerably affect the thermomechanical behavior (elastic and storage moduli, elongation to break, viscosity) of the tape and therefore the lamination process. The temperature required for a proper lamination increases from 50 up to 75°C passing from the system without rice starch to the one with the highest pore former amount. This work identifies for the first time an optimal lamination viscosity (10^{10} Pa s), regardless the tapes formulation, required for a suitable adhesion among the layers.

Keywords

Tape casting; Lamination; Viscoelasticity; Rice Starch; Barium Cerate Zirconate

1. Introduction

Tape casting is the most widely used technique for large scale fabrication of green sheets to be used in multilayer ceramic technology [1-2]. Since the 50s, tape casting has been mainly exploited for the commercial production of electronic substrates and multilayer capacitors [3-4]. In this area, the research has been applied in multilayer structures of a large variety of dielectric, ferroelectric, insulator and piezoelectric materials for electronic components such as capacitors, actuators, transducers, varistors, resistors, energy harvesters, etc. [5]. More recently, tape cast multilayer structures have been developed for structural applications [6-11], YAG-based lasers [12-14], Solid Oxide Fuel Cells [15-18], Solid Oxide Electrolysers cells [19-20], Lithium / Sodium Ion Batteries [21-23] and Gas Separation Membranes [24-27], confirming tape casting as powerful and flexible industrial technology.

The technique generally requires the following steps (Figure 1): i) slurry preparation, ii) casting and drying, iii) punching and lamination and iv) thermal treatments.

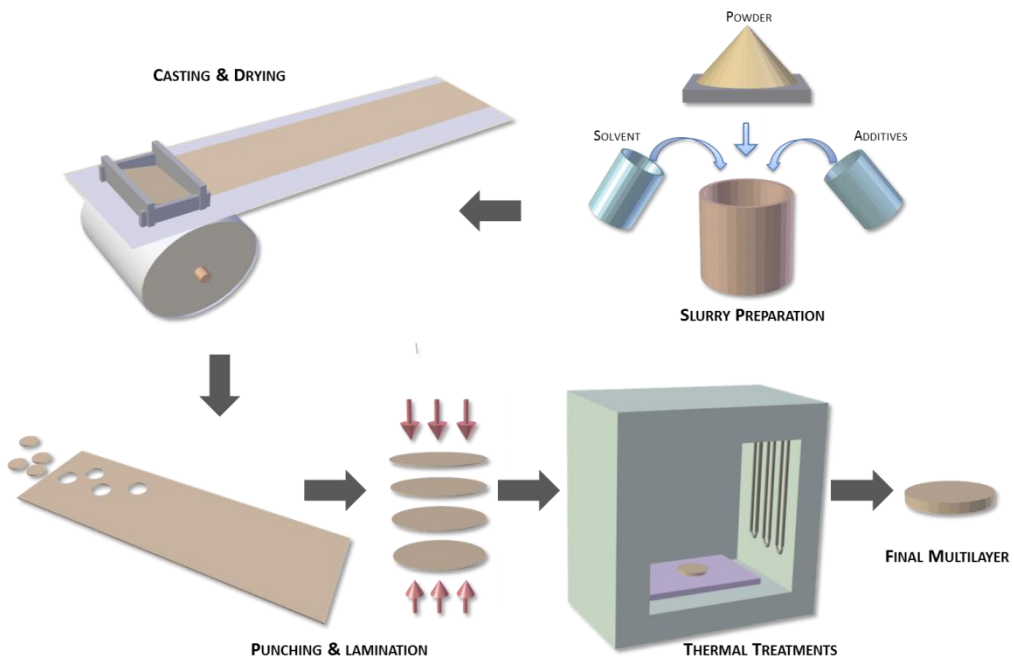

Figure 1 Production steps for the fabrication of multilayer architectures through tape casting technology.

Each step of the process must be carefully optimized in order to obtain the final multilayer product with the desired properties. The green sheets, in particular, are the fundamental building blocks for the multilayers development and need to meet several requirements to enable high quality and reliable final products.

The green ceramic tapes are generally produced starting from well-optimized slurries. These are typically prepared by dispersing the ceramic powder in a solvent with the addition of significant amounts of organic compounds (binders, plasticizers, dispersing agents and eventually pore formers and surfactants) necessary to give, after casting and solvent evaporation, flexible and crack-free tapes [28-29]. In this respect, the green tape can be considered as a polymer-ceramic composite where the mutual physicochemical interaction of the components defines the mechanical characteristics of the material in terms of elasticity, strength and toughness. These important

properties strongly affect the further processing steps: tapes handling, cutting and lamination and deformation during the thermal treatments.

The determination of the mechanical properties of the green tapes is therefore of paramount importance in order to optimize the whole ceramic process. Up to now, the mechanical properties of the green tapes have been assessed through stress-strain measurements in tensile mode to optimize tapes composition (i.e PVP-PVA-gelatin co-binder [30], binder and plasticizer content [31-34]), adjust water based suspension [35-40], asses the influence of leached cations (i.e. Ba^{2+} [41], optimize the solid loading [42-43]).

However, the complex structure and the viscoelastic behaviour of a green tape cannot be described only using static methods. The macromolecular mobility is in fact dependent upon many factors related either to the intrinsic material properties (i.e. chemical structure, molecular architecture, molecular weight and crosslinking, copolymers and blends, plasticizers, molecular orientation, fillers) and the operating conditions (i.e. time, temperature, frequency, stress or strain applied) [44]. To the authors knowledge the viscoelastic properties in terms of stiffness (modulus), ability to recover from deformation (elasticity), tendency to flow (viscosity) for green ceramic tapes have never been investigated so far. The lack of a deep understanding of the thermomechanical properties of the ceramic tapes has hindered the development of validated and standardized methods able to predict the lamination conditions necessary for the multilayers production and therefore simplify the optimization process.

In this paper we will present for the first time, the use of advanced Dynamical Mechanical Analysis (DMA), commonly used for polymer-based materials, to univocally define the lamination process conditions needed to obtain products with the suitable morphological and functional characteristics. To firstly demonstrate the potential of this technique, the characterization of proton conductive ceramic tapes based on the solid solutions of yttrium-doped barium cerate and barium zirconate (BCZY) will be presented as case study. The use of this material combined to the tape casting technology has received increasing interest in proton-conducting intermediate-temperature solid-

oxide fuel cells and electrolysers (SOFC/SOECs) [45-47] as well as in hydrogen separation membranes [48-50]. These devices are constituted by a porous/dense laminated structure where the porous layer is obtained by mixing organic or inorganic pore-forming agents into the ceramic slurry before tape casting.

In this study, the influence of the slurry formulation, in particular of the pore former content, on the thermo-mechanical properties of the tapes, will be investigated using a dynamic mechanical analyser. This work will allow to develop a characterization protocol for green tapes able to optimize the lamination process through the identification of parameters such as lamination temperature and viscosity.

2. Experimental

For the production of the tapes, BCZY powder ($BaCe_{0.65}Zr_{0.20}Y_{0.15}O_{3-\delta}$, Specific Surface Area (SSA) = 5.8 m^2/g), supplied by Marion Technology was used as starting material. Rice Starch (RS, moisture content between 7.5-13 %, Aldrich, USA), with average particle size of 5-6 μm was used as sacrificial pore forming agent.

The slurries were prepared by adding to the starting ceramic powders the desired amounts of solvent (azeotropic mixture of ethyl alcohol and methyl ethyl ketone (EtOH-MEK), Sigma–Aldrich), deflocculant (glycerinetrioleate (GTO), Fluka), binder (Butvar B98, Monsanto Co., St Louis, MO, USA) and plasticizer (Santicizer 160 Monsanto Co., St Louis, MO, USA), following the standard colloidal processing technique already described elsewhere [50]. The compositions of the green layers are reported in Table 1. The rice starch content was increased from 35 up to 50 Vol % respect to the ceramic powder, lowering the amount of the organics (binder + plasticizer) but keeping constant the binder/plasticizer ratio as well as the ceramic loading and the amount of deflocculant. The tape formulation without rice starch was considered as well for comparison. The

ball-milled suspensions were deaerated under vacuum and cast on a moving Mylar carrier (v = 6 mm/s) obtaining, after solvent evaporation, green tapes with the desired thickness (≈ 0.4 mm).

Table 1 Green tapes formulations with different amounts of rice starch as pore former. The number in the tape's name indicates the % amount of Rice Starch added in respect to the ceramic powder.

Tape	**Powder**	**Deflocculant**	**Binder**	**Plasticizer**	**Rice Starch**
	Vol %	Vol %	Vol %	Vol %	Vol %
BCZY_0	25.27	1.37	34.98	38.38	-
BCZY_35	25.27	1.37	28.49	31.26	13.62
BCZY_40	25.27	1.37	26.95	29.57	16.84
BCZY_45	25.27	1.37	25.12	27.56	20.68
BCZY_50	25.27	1.37	22.93	25.16	25.27

Figure 2 reports pictures of the tapes obtained with the formulations reported in Table 1. All the resulting tapes were defect-free.

Figure 2 Pictures of the tapes with different amount of pore former. The corresponding formulations are reported in Table 1.

The thermo-mechanical properties and the lamination conditions of BCZY green tapes with different rice starch content were evaluated through a dynamic mechanical analyzer (DMA Q800,

TA Instruments, USA), using a tension film-fiber (Fig. 3a) and a compression clamp (Fig. 3b) respectively. The experimental DMA analyses conditions and the corresponding properties evaluated are summarized in Table 2.

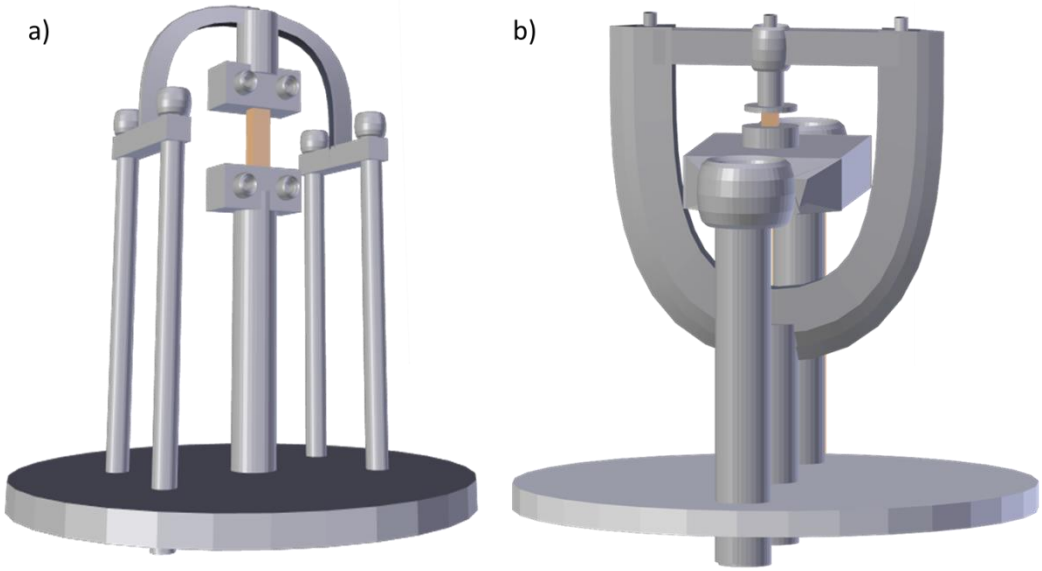

Figure 3 Scheme of the DMA clamps used in this work: tension film-fiber (a) and compression clamp.

Table 2 Summary of the experiments carried out with the DMA. The reported abbreviations stand for F_{static} (Static Force), T (Temperature), σ (Stress), ε (Strain/Elongation), f (Frequency), E' (Storage modulus), E'' (Loss Modulus), tan δ (Loss factor), t (Time), J(t) (Creep compliance) Ƞ (Viscosity) $\Delta l/l_0$ (Deformation).

Clamp	Mode	Sample shape	Operative Parameters	Properties evaluated	
Tension film - fiber	Strain rate	Dog-bone	ε = 5000-25000 μm; F_{static} = 0.01 N	σ_{max} [MPa] ε_{max} [%]	Stress, strain, yield to fracture, elastic modulus, toughness

	Multi frequency - strain	Rectangular	ε= 0.2%; f = 2 Hz; $T_{range} = T_{amb}$ – 100°C, heating rate = 3 °C/min	E' [MPa] E'' [MPa] tan δ	Determination of the moduli as functions of temperature
Compression	Creep	Squared bilayers	σ = 0.4 MPa; t = 5 min; T = 35 - 75°C	J(t) [$\mu m^2 N^{-1}$] η [Pa · s] $\Delta l/l_0$ [%]	Creep compliance, viscosity and deformation as functions of the temperature

The as-laminated DMA bilayer samples were observed with an optical microscope (Leica DM RME) to verify the quality of the lamination following the procedure reported elsewhere [51]. The adhesion among the layers was also assessed after the thermal treatment of the bilayer samples at 1450°C x 4h, following a sintering profile previously optimized [50]. The sintered bilayers cross sections were then embedded under vacuum in epoxy resin (EpoFix, Struers) and then polished down to 0.25 µm finish with an automatic polishing machine (Tegramin-25, Struers). The lamination adhesion was finally evaluated through microstructural/morphological scanning electron microscopy analyses (SEM-FEG, Carl Zeiss Sigma NTS GmbH, Oberkochen, Germany).

3. Results and Discussion

3.1 Thermomechanical behaviour of the green tapes

The effect of the pore former (rice starch) load onto the mechanical properties of BCZY green tapes was firstly investigated. The pore former amount is in fact a key variable that governs the final porosity of the ceramic layers and, therefore, the gas permeation, an important parameter for the final performances of solid oxide fuel cells/electrolyzers [52] and gas separation membranes [53]. Dog-bone samples were obtained from the different tapes and stress-strain curves were collected using the film-tension clamp at room temperature. The results show that the amount of rice starch strongly affects the elastic modulus, the elongation and stress to break (Figure 4 and Table 3).

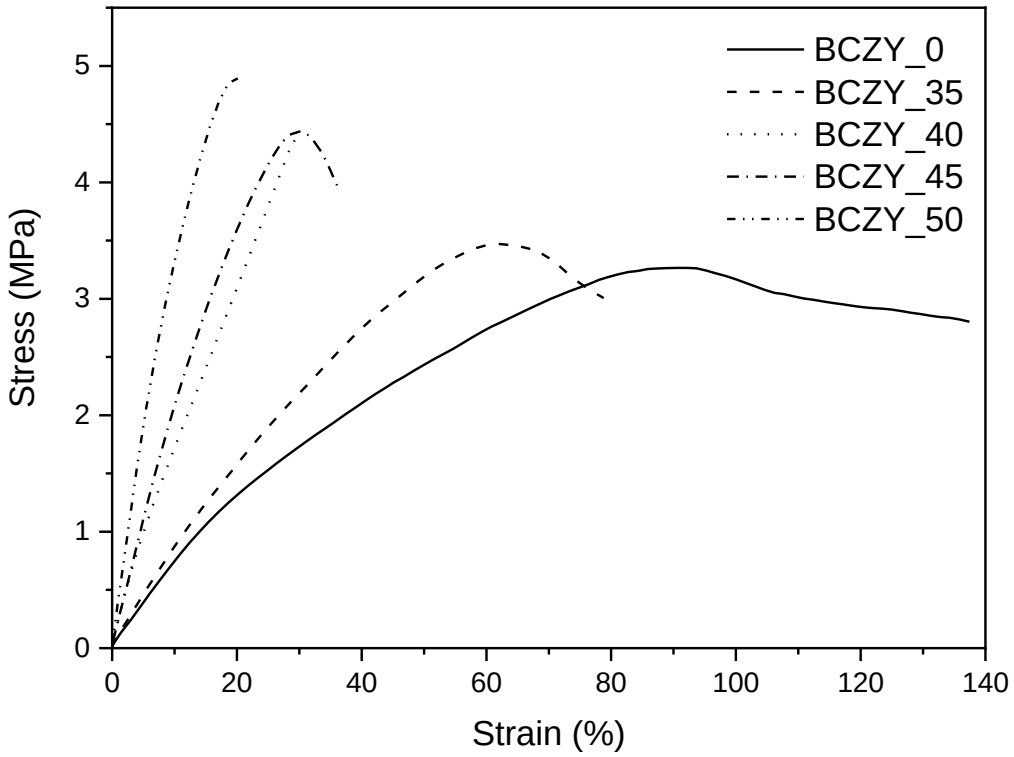

Figure 4 Stress-strain curves of the BCZY tapes with different rice starch contents.

Table 3 Mechanical properties of the green BCZY tapes as a function of the RS content.

Tape	**σ_{max}**	**Elastic modulus**	**Elongation to break**
	(MPa)	(MPa)	(%)
BCZY_0	3.4 ± 0.2	6.7 ± 0.6	133.9 ± 3.1
BCZY_35	3.5 ± 0.1	8.9 ± 0.8	76.7 ± 5.7
BCZY_40	4.2 ± 0.1	20.5 ± 1.8	58.6 ± 5.9
BCZY_45	4.3 ± 0.1	21.7 ± 0.6	33.8 ± 1.5
BCZY_50	5 ± 0.1	40.4 ± 4.2	21.2 ± 1.5

As clearly shown by Table 3, an increasing amount of pore former increases the elastic modulus of the tape. It is worth remembering, in fact, that each tape has the same volume of powder and dispersant, differing only on the % of starch and, as a consequence, of organics (binder+plasticizer).

This behaviour is related to two synergic effects: i) the blocking effect of the rice starch on the mobility of the binder polymeric chains and ii) the lower content of the binder, which results in a more rigid net. The binder provides, in fact, strength to the green tapes after the solvent evaporation through organic bridges between the ceramic particles. When there is not enough binder, the resulting green tape develops only the elastic portion of the stress-strain curve.
This is confirmed by the results showed in Figure 5a, were elastic moduli decreases with an increase of the binder content.

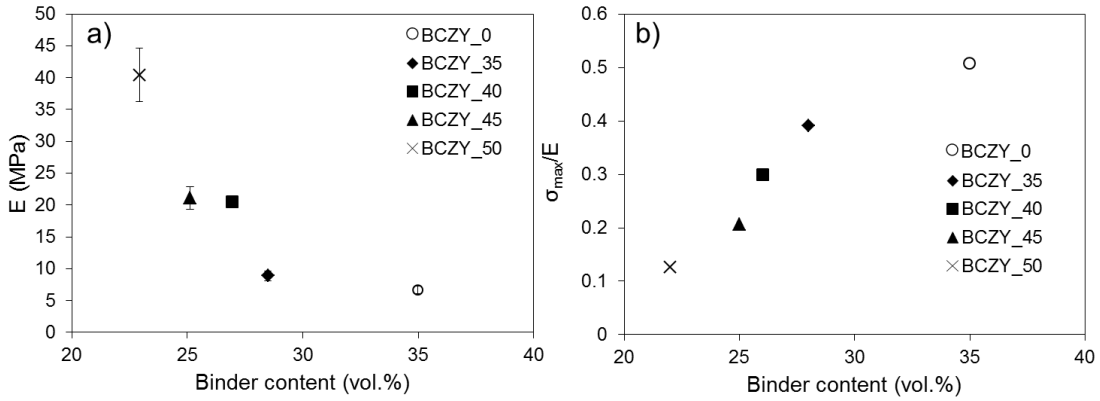

Figure 5 Elastic modulus(E) (a) and (σ_{max}/E) (b) values as a function of the binder content. Standard deviations are also reported in (a), while in (b) standard deviation indicators are smaller than the symbols.

In literature, one of the parameters used for estimating the tape toughness is the tensile strength/elastic modulus ratio (σ_{max}/E) [54-55]. High ratio values mean high fracture toughness and therefore good crack resistance. Figure 5b shows the σ_{max}/E values as a function of the binder content for the tapes with different amount of pore former. The σ_{max}/E ratio increases raising the binder content, confirming again its role into the polymer-ceramic composite for the formation of a macromolecular network with the suitable mechanic-physical properties. However, it is worth to notice that, even if the substitution of binder with rice starch greatly affects the elongation to break parameter, the mechanical properties in terms of E and σ_{max}/E are only slightly influenced when the

lowest amount of pore former is introduced into the tape (BCZY_35). This might be due to a compensation-synergic behaviour of the polymeric components i.e. binder and pore former.

All the previous tests confirmed that at room temperature the organic pore former increases the elastic modulus of the tape acting like an inorganic, ceramic fraction rather than an organic component as it should be expected considering its chemical nature. Rice starch is as a matter of fact a polymer, therefore its thermomechanical properties may vary with temperature, i.e. during the lamination process. In particular, it is a semicrystalline polymer in which crystalline regions are interspersed into a continuous amorphous matrix [56]. On heating or plasticizer addition (i.e. moisture) the mobility of the amorphous part increases, and the material becomes more flexible or rubbery. However, the molecular motion of starch, which defines its glass transition temperature (T_g), is hindered by cohesive forces along and between the chains. The crystalline regions of the polymer act in fact as physical cross-linkers that add rigidity to the amorphous region having an effect similar to that of chemical cross-links [56].

The effect of temperature on the behaviour of tapes with rice starch is therefore very important to assess its role onto the green mechanical properties. For this purpose, rectangular samples were cut from the different tapes and a sinusoidal stress was applied increasing the temperature, measuring the resulting oscillating sinusoidal strain. Figure 6 shows the temperature-dependence of the storage modulus (i.e. the elastic part of the polymer) recorded in the as-mentioned dynamic mode. The trend obtained with the dynamic application load agrees with the results previously discussed for the tensile tests: for an increasing amount of pore former the storage modulus of the tape increases in the whole temperature range considered. In particular, the graph underlines that the tape without pore former has E' values similar to the ones registered for the sample with the lowest amount of RS (BCZY_35) up to about 75°C. At higher temperatures however, the softening of the binder-plasticizer network of the BCZY_0 tape becomes predominant due to the lack of RS acting as cross-linker. The crystalline regions of the latter in fact, for which the melting transition is above 95°C depending on the moisture content [57], probably promote the rigidity of the tape. In addition, the

higher the rice starch content, the more E' varies with the temperature. For example, BCZY_50 has an E' value of 131 MPa at 40°C which decreased to 43 MPa at 100°C; while the E' of the BCZY_40 decreased from 57 MPa to 11 MPa in the same temperature range (note that the y-scale of Figure 6 is logarithmic). This behaviour is probably ascribed to the activation (softening) of the amorphous parts of starch above the T_g that occurs in the 50-70°C temperature range depending on the moisture content [57-58].

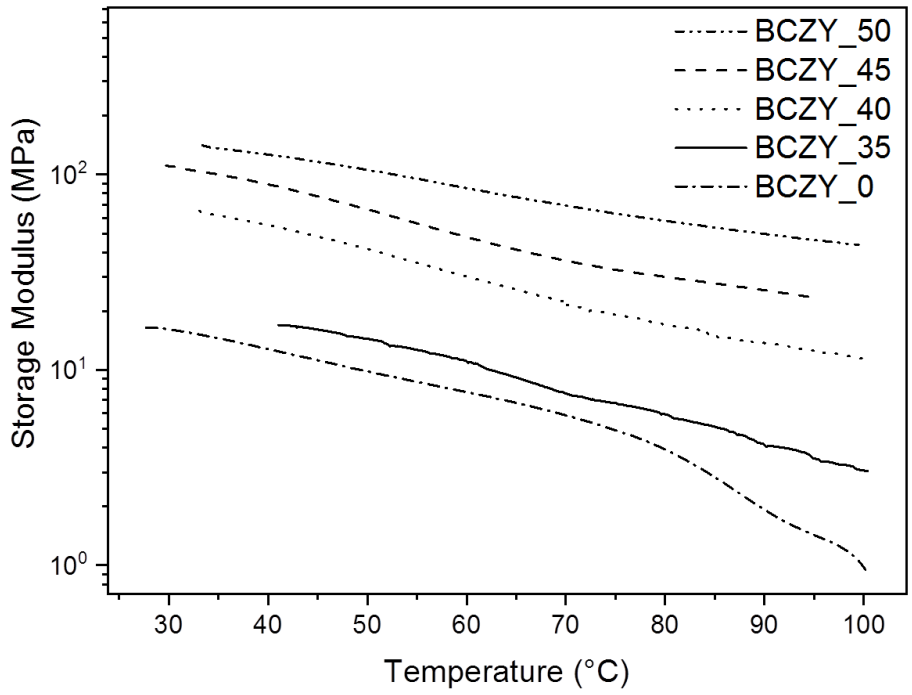

Figure 6 Storage modulus (E') of the different tapes as a function of temperature.

As explained at the beginning of this paragraph, the optimization of the lamination parameters is extremely important in order to obtain a multilayer without deformation and/or mass loss. This process is strictly related to the viscosity of the tape and in particular to the mobility of the macromolecular chains, responsible for the tape's lamination/adhesion. Therefore, viscosity values of each tape were calculated from the creep measurements at different temperatures (Table 4).

The viscosity values for the formulation with the highest amount of RS (BCZY_50) are not reported. Their corresponding registered creep curves, in fact, have a negative slope due to the slipping of the sample from the clamp during the tests as a consequence of a plasticizer release in temperature [59].

Table 4 Viscosities values obtained from creep tests at different temperatures.

	Ƞ [Pa· s] · 10^9		
Temperature (°C)	**40**	**50**	**60**
BCZY_0	7.2 ± 1.4	1.3 ± 0.2	0.4 ± 0.1
BCZY_35	14.2 ± 4.1	1.4 ± 0.2	0.4 ± 0.1
BCZY_40	20.2 ± 2.9	2.6 ± 0.7	0.7 ± 0.1
BCZY_45	31.3 ± 17.6	8.1 ± 1.4	1.6 ± 0.2

Viscosity values have the same trend of the storage modulus (Figure 6): the higher the starch content the higher the viscosity and the highest is its variation with temperature. A less temperature-dependence of viscosity for tapes without or with low starch content was in fact registered in the investigated temperatures range, confirming therefore the importance of the lamination process optimization.

These results confirm that the pore former content considerably affects the thermomechanical behaviour of the material, with predictable implications on the lamination process.

3.2 Mimic of the Lamination Process

The optimization of the lamination parameters is a key step for the production of a multilayer. The previous results allowed to obtain useful correlations between composition and elastic/storage modulus or viscosity as a function of temperature. To directly correlate these results with the actual lamination process, a new innovative experimental set-up was designed: two rectangular samples cut off from the tapes were stacked and inserted between the plates of the compression clamp of the

DMA. This new configuration was used to directly measure the bilayer deformation (in terms of strain and shrinkage along the thickness), creep compliance and viscosity under a given pressure and temperature, mimicking the actual lamination process.

The strain and the creep compliance of two stacked layers for BCZY_0 tape with the temperature are correlated in Figure 7. Optical microscope images are also reported to assess the lamination condition after each test. The results obtained for the other two stacked layers of BCZY_35, BCZY_40, BCZY_45, BCZY_50 are reported in Appendices (A.1, A.2, A.3, A.4 respectively).

In general there is an increase in strain with temperature, that means a sample's thickness reduction induced by a definite mass flow while a pressure is applied. For an effective lamination the creep compliance should increase so that less force is needed to deform the material. In particular, this analysis confirmed that the lamination temperature increases from 50 up to 75°C passing from the system without rice starch to the one with the highest amount of pore former. For higher lamination temperatures, the strain and, therefore, the shrinkage increases enhancing the probability of multilayer deformation. This is perfectly in line with the considerations previously done on the thermomechanical behaviour of each single tape with different amount of organics.

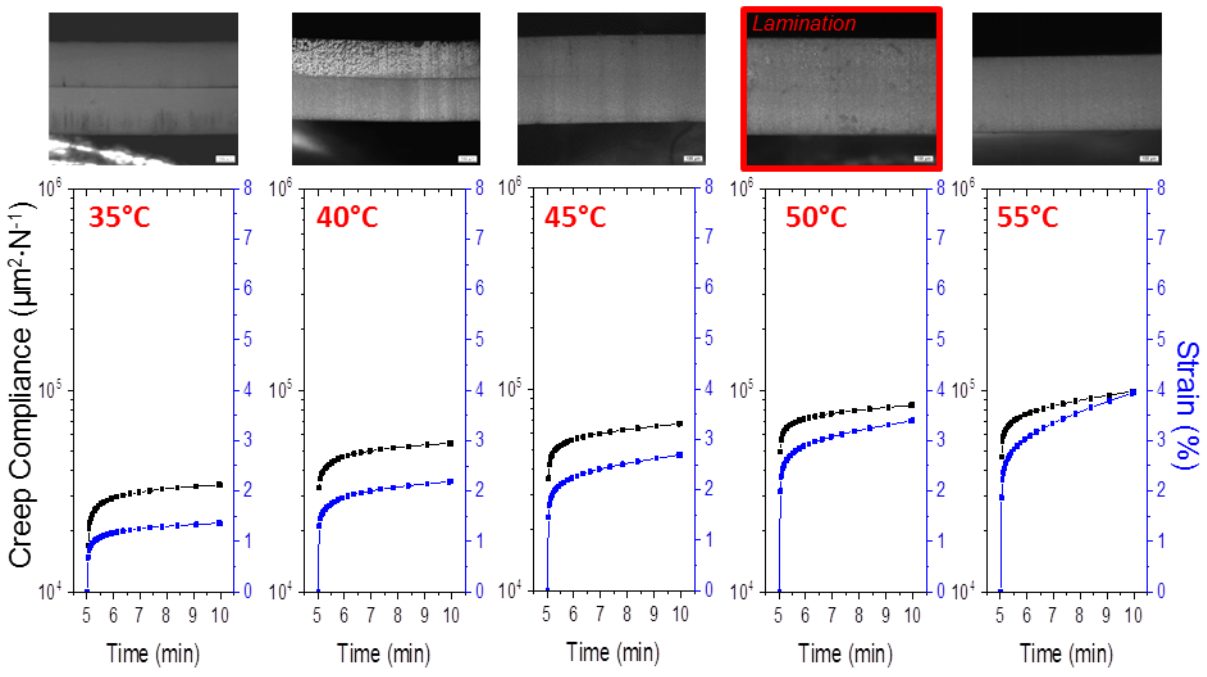

Figure 7 Creep compliance and stain values at different temperatures of the tape BCZY_0. Optical microscope images of the sample after each test are reported above.

For each creep test on the bilayers, the viscosity as well as the shrinkage along the thickness were determined at the different temperatures. The shrinkage values, in particular, were calculated considering the strain values registered at the end of the creep test at each temperature (Figures 7, A.1-A.4):

$$\text{Shrinkage (\%)} = \frac{L_f - L_0}{L_0} * 100$$

Where, L_0 and L_f are the sample thickness before and after creep test, respectively.

Figure 8 shows how the temperature and rice starch content affect the viscosity (Fig. 8a) and the shrinkage (Fig. 8b) for each system evaluated. The results obtained confirm the ones previously discussed on the thermomechanical behaviour of each tape. The viscosities decrease with the increase in temperature. On the other hand, the absolute values of viscosity calculated for each bilayer are comparable but shifted at higher temperatures by increasing the pore former content as previously observed for the single tape, confirming again the blocking effect of RS. Note that a viscosity value discontinuity was registered for BCZY_50 in the 60-70 °C temperature range. Even if this behaviour is probably linked to the softening of the amorphous parts of starch that is present, in this formulation, in large amount, further investigations will be needed to fully understand this phenomenon.

Finally, the trend of the shrinkage follows the one of viscosity: changes in viscosity imply changes in the material's shrinkage and thus in the lamination of the bilayers.

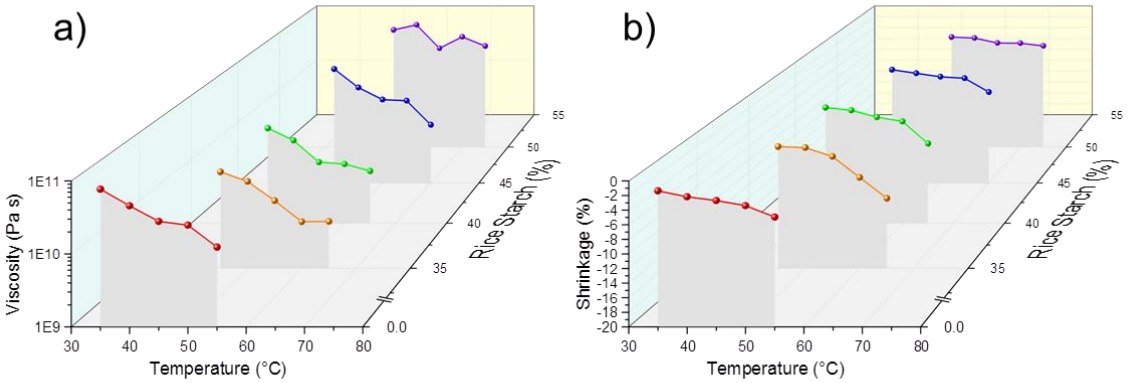

Figure 8 Viscosity a) and shrinkage b) values calculated after each creep test at different temperatures for all the bilayers analysed.

Figure 9 reports the optimal lamination parameters in terms of lamination viscosity and $T_{lamination}$ determined from the previously described creep tests for each system. The reported correlations demonstrate that the lamination process is hindered by the presence of rice starch: the pore former in fact increases the viscosity of the tape making the lamination process more difficult.

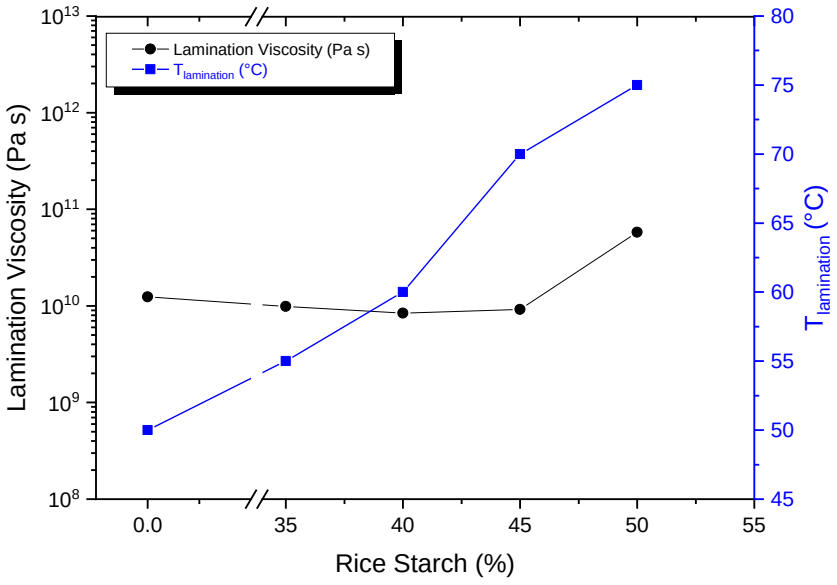

Figure 9 Lamination viscosity and lamination temperature trends as a function of the rice starch content.

It is important to notice that the tapes show similar values of lamination viscosity (10^{10} Pa s). This result seems to indicate that it is possible to identify a common value of viscosity necessary to obtain an effective lamination. The discrepancy showed by BCZY_50 is ascribed to the high level of pore former in the system that substitutes the binder-plasticizer network. This tape was in fact theoretically formulated to complete the series of samples with incremental RS, following the logic approach reported in the experimental part, with the aim to be comparable with the other formulations and thus understanding the influence of pore former. A fully optimization of this tape, in terms of balacing of organics amount, should be necessary if considered for the further processing steps and practical applications.

In order to assess the influence of the lamination temperature on the final adhesion between the layers, the different bilayers were sintered at 1450°C x 4h, and the resulting cross sections investigated by SEM analyses. The SEM micrographs reported in Figure 10 show that the optimization of the lamination condition is crucial for the adhesion of the multilayers even after the sintering process. No delamination defects were in fact detected for bilayers properly laminated at the temperatures equal to the optimal ones as derived from the study on the lamination process previously described in Figure 9.

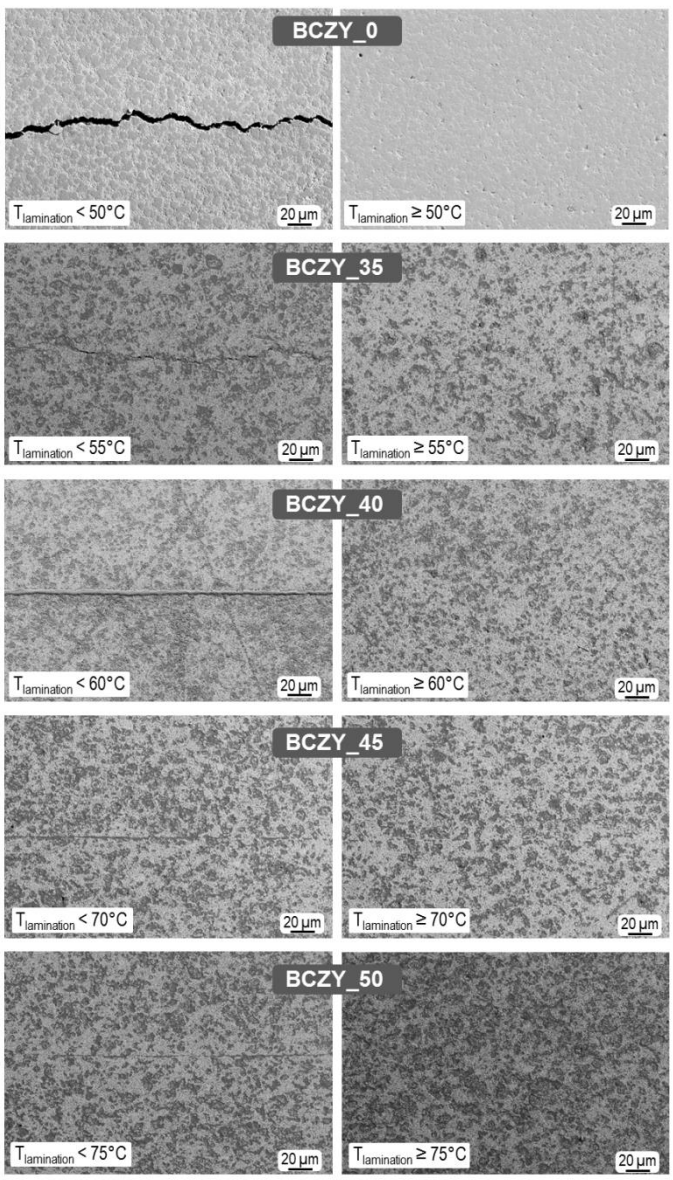

Figure 10 Effect of the lamination temperatures on the sintered bilayers with different amount of rice starch.

Conclusions

This work explored for the first time the possibility to use Dynamic Mechanical Analysis as a powerful tool to characterize and design green tapes and multilayers for energy applications. DMA allowed to find helpful results correlating the formulation of the tapes with their thermomechanical behaviour and then with the lamination process.

In particular, it was found that the rice starch, used as pore former, has a ceramic particle-like blocking effect on the chain mobility at low temperature. Temperature-programmed static and dynamic experiments assessed however the temperature-dependence of the rice starch blocking effect on storage modulus and viscosity.

Exploiting a compressive-mode experimental set-up, the lamination process was successfully mimicked and investigated. The main results show that the viscosity, strain and shrinkage along the bilayer thickness are strongly affected by the temperature and the rice starch content. As a consequence, the optimal lamination temperature for each system strongly differs with the tape formulation, increasing from 50 up to 75°C rising the rice starch amount. For the first time, an optimal lamination viscosity (10^{10} Pa s) required for a suitable adhesion among the layers was individuated. Even if more research has to be done to confirm this result, the possibility to identify a unique parameter defining the best conditions for lamination represents an important breackthrough for the multilayers technology field.

Conflicts of interest

There are no conflicts of interest to declare.

Acknowledgements

This work was funded by the agreement between the Italian Ministry of Economic Development and the Italian National Research Council ‘‘Ricerca di sistema elettrico”, under the frame of the Project: “Materiali di frontiera per usi energetici”.

Appendix A. Supplementary data

Supplementary material related to this article can be found in the online version.

References

[1] H. Hellebrant, Tape casting. In Processing of Ceramics, Part 1, ed. R. J. Brook. Materials Science and Technology, Vol 17A. VCH Verlagsgesellschaft, Weinheim, FRG, 1996, pp. 189–265.

[2] R. E. Mistler, Tape-casting: the basic process for meeting the needs of electronics industry, Am. Ceram. Soc. Bull. 69 (1990) 1022-1026.

[3] G.N. Howatt, R.G. Breckenridge, J.M. Brownlow, Fabrication of thin ceramic sheets for capacitors, J. Am. Ceram. Soc. 30 (1947) 237-242.

[4] G.N. Howatt, Method of Producing High Dielectric High Insulation Ceramic Plates, US Patents No. 2582993 (January 1952).

[5] R.E. Mistler, E.R. Twiname, Tape Casting Theory and Practice, The American Ceramic Society, Westerville, OH, 2000.

[6] L. Cheng, M. Sun, F. Ye, Y. Bai, M. Li, S. Fan, L. Zhang, Structure design, fabrication, properties of laminated ceramics: A review, Int. J. Lightweight Mater. Manufact. 1 (2018) 126-141. https://doi.org/10.1016/j.ijlmm.2018.08.002

[7] T. Lube, J. Pascual, F. Chalvet, G. de Portu, Effective fracture toughness in Al_2O_3–Al_2O_3/ZrO_2 laminates, J. Eur. Ceram. Soc. 27 (2007) 1449–1453. https://doi.org/10.1016/j.jeurceramsoc.2006.04.063

[8] S. Liu, F. Ye, H. Yang, Q. Liu, B. Zhang, S. Hu, Y. Gao, W. Liu, Fabrication and properties of SiC/Si_3N_4 multilayer composites with different layer thickness ratios by aqueous tape casting, Ceram. Int. 41 (2015) 12917–12922. https://doi.org/10.1016/j.ceramint.2015.06.133

[9] Y. Bai, Y. Ma, M. Sun, S. Fan, L. Cheng, Strong and tough ZrB_2 materials using a heterogeneous ceramic–metal layered architecture, J. Am. Ceram. Soc. 102 (2019) 5013-5019. https://doi.org/10.1111/jace.16424

[10] Y. Bai, Y. Ma, M. Sun, L. Cheng, S. Fan, Sintering temperature effect on microstructure, mechanical and electrical properties of multi-layered ZrB_2-based ceramics with thin Ti interlayer, J. Eur. Ceram. Soc. 39 (2019) 3938–3948. https://doi.org/10.1016/j.jeurceramsoc.2019.06.005

[11] L.Y. Xiang, L.F. Cheng, Fabrication and mechanical properties of laminated HfC–SiC/BN ceramics, J. Eur. Ceram. Soc. 34 (2014) 3635-3640. https://doi.org/10.1016/j.jeurceramsoc.2014.04.021

[12] H. Zhao, F. Tang, Y. Xie, Z. Wen, K. Tian, X. Nie, Y. Cao, D. Tang, Fabrication and rheological behavior of tape-casting slurry for ultra-thin multilayer transparent ceramics, Int. J. Appl. Ceram. Technol. 17 (2020) 1255–1263. https://doi.org/10.1111/ijac.13421

[13] J. Hostaša, A. Piancastelli, G. Toci, M. Vannini, V. Biasini, Transparent layered YAG ceramics with structured Yb doping produced via tape casting, Opt. Mater. 65 (2017) 21-27. https://doi.org/10.1016/j.optmat.2016.09.057

[14] R. Belon, R. Boulesteix, P.M. Geffroy, A. Maître, C. Sallé, T. Chartier, Tape casting of multilayer YAG-Nd:YAG transparent ceramics for laser applications: Study of green tapes properties, J. Eur. Ceram. Soc. 39 (2019) 2161–2167. https://doi.org/10.1016/j.jeurceramsoc.2019.01.038

[15] M. Liu, Y. Liu, Multilayer tape casting of large-scale anode-supported thin-film electrolyte solid oxide fuel cells, Int. J. Hydrogen Energ. 44 (2019) 16976-16982. https://doi.org/10.1016/j.ijhydene.2019.04.161

[16] X. Chen, W. Ni, X. Du, Z. Sun, T. Zhu, Q. Zhong, M. Han, Electrochemical property of multi-layer anode supported solid oxide fuel cell fabricated through sequential tape-casting and co-firing, J. Mater. Sci. Technol. 35 (2019) 695-701. https://doi.org/10.1016/j.jmst.2018.10.015

[17] L.S. Mahmud, A. Muchtar, M.R. Somalu, Challenges in fabricating planar solid oxide fuel cells: A review, Renew. Sust. Energ. Rev. 72 (2017) 105-116. https://doi.org/10.1016/j.rser.2017.01.019

[18] A. Lanzini, C. Guerra, P. Leone, M. Santarelli, F. Smeacetto, S. Fiorilli, A. Gondolini, E. Mercadelli, A. Sanson, N.P. Brandon, Influence of the microstructure on the catalytic properties of SOFC anodes under dry reforming of methane, Mater. Lett. 164 (2016) 312–315. https://doi.org/10.1016/j.matlet.2015.10.171

[19] J. Zhou, Z. Ma, L. Zhang, C. Liu, J. Pu, X. Chen, Y. Zheng, S.H. Chan, Study of CO_2 and H_2O direct co-electrolysis in an electrolyte-supported solid oxide electrolysis cell by aqueous tape casting technique, Int. J. Hydrogen Energ. 44 (2019) 28939-28946. https://doi.org/10.1016/j.ijhydene.2019.09.141

[20] A. Gondolini, E. Mercadelli, P. Pinasco, C. Zanelli, C. Melandri, A. Sanson, Alternative production route for supporting $La_{0.8}Sr_{0.2}MnO_{3-\delta}$-$Ce_{0.8}Gd_{0.2}O_{2-\delta}$ (LSM-GDC), Int. J. Hydrogen Energ. 37 (2012) 8572-8581. https://doi.org/10.1016/j.ijhydene.2012.02.091

[21] Z. Jiang, S. Wang, X. Chen, W. Yang, X. Yao, X. Hu, Q. Han, H. Wang, Tape-Casting $Li_{0.34}La_{0.56}TiO_3$ Ceramic Electrolyte Films Permit High Energy Density of Lithium-Metal Batteries, Adv. Mater. 32 (2020) 1906221. https://doi.org/10.1002/adma.201906221

[22] V.A. Vizgalov, A.R. Lukovkina, D.M. Itkis, L.V. Yashina, Tape-casted liquid-tight lithium-conductive membranes for advanced lithium batteries, J. Mater. Sci. 54 (2019) 8531–8541. https://doi.org/10.1007/s10853-019-03463-2

[23] K. Okubo, H. Wang, K. Hayashi, M. Inada, N. Enomoto, G. Hasegawa, T. Osawa, H. Takamura, A dense NASICON sheet prepared by tape-casting and low temperature sintering, Electrochim. Acta 278 (2018) 176-181. https://doi.org/10.1016/j.electacta.2018.05.020

[24] F. Schulze-Küppers, S. Baumann, W.A. Meulenberg, H.J.M. Bouwmeester, Influence of support layer resistance on oxygen fluxes through asymmetric membranes based on perovskite-type oxides $SrTi_{1-x}Fe_xO_{3-\delta}$, J. Membr. Sci. 596 (2020) 117704. https://doi.org/10.1016/j.memsci.2019.117704

[25] C. Li, X. Ban, C. Chen, Z. Zhan, Sandwich-like symmetric dual-phase composite membrane with an ultra-thin oxygen separation layer and excellent durability, Solid State Ion. 345 (2020) 1151762. https://doi.org/10.1016/j.ssi.2019.115176

[26] E. Mercadelli, A. Gondolini, D. Montaleone, P. Pinasco, S. Escolástico, J.M. Serra, A. Sanson, Production strategies of asymmetric $BaCe_{0.65}Zr_{0.20}Y_{0.15}O_{3-\delta}$–$Ce_{0.8}Gd_{0.2}O_{2-\delta}$ membrane for hydrogen separation, Int. J. Hydrogen En. 45 (2020) 7468-7478. https://doi.org/10.1016/j.ijhydene.2019.03.148

[27] D. Montaleone, E. Mercadelli, S. Escolàstico, A. Gondolini, J. M. Serra, A. Sanson, All-ceramic asymmetric membranes with superior hydrogen permeation, J. Mater. Chem. A, 6 (2018) 15718. https://doi.org/10.1039/C8TA04764B

[28] E. Mercadelli, A. Sanson, P. Pinasco, E. Roncari, C. Galassi, Influence of carbon black on slurry compositions for tape cast porous piezoelectric ceramics, Ceram. Int. 37 (2011) 2143–2149. https://doi.org/10.1016/j.ceramint.2011.03.058

[29] E. Mercadelli, A. Gondolini, P. Pinasco, A. Sanson, Stainless Steel Porous Substrates Produced by Tape Casting, Met. Mater. Int. 23 (2017) 184–192. https://doi.org/10.1007/s12540-017-6336-2

[30] D.J. Kim, I.S. Park, M.H. Lee, Tensile strength of aqueous-based alumina tapes using a PVP–PVA–gelatin cobinder, Ceram. Int. 31 (2005) 577-581. https://doi.org/10.1016/j.ceramint.2004.07.006

[31] S.A. Uhland, R.K. Holman, S.M. Collier, M.J. Cima, E.M. Sachs, Strength of Green Ceramics with Low Binder Content, J. Am. Ceram. Soc., 84 (2001) 2809–2818. DOI:10.1111/j.1151-2916.2001.tb01098.x

[32] T. Xie, S. Jiang, M. Fan, Improvement on the mechanical properties of zinc oxide green sheets by aqueous acrylamide gel tape casting, Ceram. Int. 35 (2009) 2645–2649. https://doi.org/10.1016/j.ceramint.2009.02.029

[33] D.H. Kim, K.Y. Lim, U. Paik, Y.G. Jung, Effects of chemical structure and molecular weight of plasticizer on physical properties of green tape in $BaTiO_3$/PVB system, J. Eur. Ceram. Soc. 24 (2004) 733–738. https://doi.org/10.1016/S0955-2219(03)00256-5

[34] M. Fu, T. Xie, S. Jiang, Rheology and physical properties of $Bi_{0.5}(Na_{0.82}K_{0.18})_{0.5}TiO_3$ piezoelectric thick films by aqueous gel-tape casting process, Ceram. Int. 35 (2009) 2463–2467. https://doi.org/10.1016/j.ceramint.2009.02.014

[35] D.H. Yoon, B.I. Lee, Processing of barium titanate tapes with different binders for MLCC applications—Part II: Comparison of the properties, J. Eur. Ceram. Soc. 24 (2004) 753–761. https://doi.org/10.1016/S0955-2219(03)00334-0

[36] Y. Zhang, C. Qin, J. Binner, Processing multi-channel alumina membranes by tape casting latex-based suspensions, Ceram. Int. 32 (2006) 811–818. https://doi.org/10.1016/j.ceramint.2005.06.005

[37] F. Doreau, G. Tarì, M. Guedes, T. Chartier, C. Pagnoux, J.M.F. Ferreira, Mechanical and Lamination Properties of Alumina Green Tapes Obtained by Aqueous Tape-casting, J. Eur. Ceram. Soc. 19 (1999) 2867-2873. https://doi.org/10.1016/S0955-2219(99)00052-7

[38] C.A. Gutièrrez, R. Moreno, Influence of slip preparation and casting conditions on aqueous tape casting of Al_2O_3, Mater. Res. Bull. 36 (2001) 2059–2072. https://doi.org/10.1016/S0025-5408(01)00683-3

[39] M.P. Albano, L.B. Garrido, Influence of the slip composition on the properties of tape-cast alumina substrates, Ceram. Int. 31 (2005) 57–66. https://doi.org/10.1016/j.ceramint.2004.03.035

[40] J.H. Feng, F. Dogan, Aqueous processing and mechanical properties of PLZT green tapes, Mater. Sci. Eng. A, 283 (2000) 56-64. https://doi.org/10.1016/S0921-5093(00)00701-2

[41] D.H. Yoon, B.I. Lee, Effects of Excess Barium Ions on Aqueous Barium Titanate Tape Properties, J. Am. Ceram. Soc. 87 (2004) 1066–1071. https://doi.org/10.1111/j.1551-2916.2004.01066.x

[42] M.D. Snel, F. Snijkers, J. Luyten, A. Kodentsov, G. de With, Tape casting and reaction sintering of titanium–titanium oxide–nickel oxide mixtures, J. Eur. Ceram. Soc. 28 (2008) 1185-1190. DOI: 10.1016/j.jeurceramsoc.2007.11.001

[43] S. Li, Q. Zhang, H. Yang, D. Zou, Fabrication and characterization of $Li_{1+x-y}Nb_{1-x-3y}Ti_{x+4y}O_3$ substrates using aqueous tape casting process, Ceram. Int. 35 (2009) 421–426. https://doi.org/10.1016/j.ceramint.2007.12.003

[44] L. Gargallo, D. Radic, Viscoelastic Behaviour of Polymer, in Polymers in Physicochemical Behavior and Supramolecular Organization of Polymers, Springer Netherlands, 2009, eBook ISBN 978-1-4020-9372-2, pp 43-162.

[45] J.M. Serra, Electrifying chemistry with protonic cells, Nat. Energy 4 (2019) 178-179. https://doi.org/10.1038/s41560-019-0353-y

[46] M.P. Carpanese, M. Viviani, E. Mercadelli, A. Sanson, A. Barbucci, M. Panizza, Study of a reversible SOFC/SOEC based on a mixed anionic-protonic conductor, J. Appl. Electrochem. 45 (2015) 657-665. https://doi.org/10.1007/s10800-015-0838-8

[47] E. Mercadelli, A. Gondolini, P. Pinasco, A. Sanson, S. Barison, M. Fabrizio, Key Issues in Processing Metal-Supported Proton Conducting Anodes For SOFC Applications, ECS Transactions 35 (2011) 1761-1769. https://doi.org/10.1149/1.3570164

[48] D. Montaleone, E. Mercadelli, A. Gondolini, M. Ardit, P. Pinasco, A. Sanson, Role of the sintering atmosphere in the densification and phase composition of asymmetric BCZY-GDC composite membrane, J. Eur. Ceram. Soc. 39 (2019) 21–29. https://doi.org/10.1016/j.jeurceramsoc.2018.01.043

[49] D. Montaleone, E. Mercadelli, A. Gondolini, P. Pinasco, A. Sanson, On the compatibility of dual phase $BaCe_{0.65}Zr_{0.2}Y_{0.15}O_3$-based membrane for hydrogen separation application, Ceram. Int. 43 (2017) 10151–10157. https://doi.org/10.1016/j.ceramint.2017.05.039

[50] E. Mercadelli, D. Montaleone, A. Gondolini, P. Pinasco, A. Sanson, Tape-cast asymmetric membranes for hydrogen separation, Ceram. Int. 43 (2017) 8010–8017. https://doi.org/10.1016/j.ceramint.2017.03.099

[51] E. Mercadelli, A. Sanson, P. Pinasco, E. Roncari, C. Galassi, Tape cast porosity-graded piezoelectric ceramics, J. Eur. Ceram. Soc. 30 (2010) 1461-1467. https://doi.org/10.1016/j.jeurceramsoc.2009.12.004

[52] N. Hedayat, Y. Du, H. Ilkhani, Review on fabrication techniques for porous electrodes of solid oxide fuel cells by sacrificial template methods, Renew. Sust. Energ. Rev. 77 (2017) 1221-1239. https://doi.org/10.1016/j.rser.2017.03.095

[53] C. Gaudillere, J. Garcia-Fayos, J.M. Serra, Enhancing oxygen permeation through hierarchically-structured perovskite membranes elaborated by freeze-casting, J. Mater. Chem. A, 2 (2014) 3828–3833. https://doi.org/10.1039/C3TA14069E

[54] T. Xie, S. Jiang, M. Fan, Improvement on the mechanical properties of zinc oxide green sheets by aqueous acrylamide gel tape casting, Ceram. Int. 35 (2009) 2645–2649. https://doi.org/10.1016/j.ceramint.2009.02.029

[55] N.H. Parikh, S.C. Porter, B.D. Rohera, Tensile properties of free films cast from aqueous ethylcellulose dispersions, Pharm Res. 10 (1993) 810-815. https://doi.org/10.1023/A:1018992607245

[56] K.J. Zeleznak, R.C. Hoseney, The glass transition in starch, Cereal Chem. 64 (1987) 121-124.

[57] C.G. Biliaderis, C.M. Page, T.J. Maurice, B.O. Juliano, Thermal characterization of rice starches: A polymeric approach to phase transitions of granular starch, J. Agric. Food Chem. 34 (1986) 6-14.

[58] H.J. Chung, E.J. Lee, S.T. Lim, Comparison in glass transition and enthalpy relaxation between native and gelatinized rice starches, Carbohydr. Polym. 48 (2002) 287-298. https://doi.org/10.1016/S0144-8617(01)00259-4

[59] A. Sanson, E. Mercadelli, A. Gondolini, P. Pinasco, Unconventional Approaches for the Production of Large Area SOFC, ECS Transactions 57 (2013) 717-726. https://doi.org/10.1149/05701.0717ecst